15 Aug 2008, 11:00am - 12:30pm

Characterization of the Shear-Induced Potential (SIP) in Clay and the Application to Landslide Sites

Koichi Nakagawa
Osaka City University, Osaka, Japan

Shigenobu Yamada
Yanmar Co. Ltd., Osaka, Japan

Isamu Tsuka
NTT DATA Corporation, Tokyo, Japan


6th International Conference on
Case Histories in Geotechnical Engineering, Arlington, VA, August 11-16, 2008

CHARACTERIZATION OF THE SHEAR-INDUCED POTENTIAL (SIP) IN CLAY AND THE APPLICATION TO LANDSLIDE SITES

Koichi NAKAGAWA
Osaka City University
3-3-138 Sugimoto, Sumiyoshi-ku
Osaka 558-8585, Japan

Shigenobu YAMADA
Yanmar Co. Ltd.
1-32, Chayamachi, Kita-ku
Osaka 530-8311, Japan

Isamu TSUKA
NTT DATA Corporation
Toyosu Center Bldg., 3- 3-3 Toyosu,
Koto-ku, Tokyo 135-6033, Japan

ABSTRACT

Electrical polarizations were observed in common fine soil aggregates in shear deformation tests and simulations conducted in a laboratory. This electric potential is called Shear-induced Potential (SIP). The SIP can be interpreted as the physicochemical interaction between the surface of clay particles and interstitial water by the kinetics of the electric double layer. The SIP could not be detected in a remolded craft clay sample, which was possibly treated with electrically non-dipole oil. In the laboratory, a plane strain test under the un-drained condition was carried out to reveal the characteristics of the polarization accompanying the shear deformation. Gouges from the active faults were remolded with saline water and consolidated axially under the condition of K_0 as the test specimen. The polarities of the electric charges induced at the surfaces of the specimens were positive, neutral and negative for the maximum (tensional), intermediate and minimum principal strain axial planes, respectively. In addition, in-situ observations of the spontaneous potential (SP) were performed at gravitationally unstable sites to verify the results obtained in the laboratory. The characteristic distributions of the charge and time variation of SP were consistent with the pattern observed by the scaled model experiments in the laboratory.

INTRODUCTION

It is known that electric forces work between clay particles through electrolytic pore water. Coupling between the electrical and hydraulic flow gradients is responsible for four electrokinetic phenomena (electroosmosis, streaming potential, electrophoresis and migration or sedimentation potential) in materials such as fine-grained soils, where the charged particles are balanced by mobile countercharges (Mitchell, 1993). The concentration of electrolytes in pore water changed during compaction in laboratory compression tests (e.g., Kazintsef, 1968; Sawabini et al., 1972). In general, consolidation is presumed to strengthen the inter-particle bonding in soil systems. Consequently, the stiffness or strength of the soil increases with the decreasing void ratio and with elapsed time in the stage of secondary compression. In the secondary compression, while the grains approach together, the dissolved ions move through the pore water to achieve electric equilibrium of the interface (Nakagawa et al., 1995). The equilibrium, however, is assumed to be lost by rearrangement of the grains through shear deformation. The loss of equilibrium results in electric polarization of the substance. Accordingly, the electric potential can become a good indicator of the shear strain. As a practical application, monitoring the electric potential may indicate a symptom of failure, such as a landslide or fault sliding. However, a systematic study on the relationship between shear strain and electrical property in fine aggregates has not yet been conducted. In contrast, there are many studies on the situ measurements of SP (spontaneous potential) to obtain evidence of the streaming potential or symptoms of an earthquake.

PLANE STRAIN SHEAR TEST

A simple shear plane test was performed in the laboratory to examine the relationship between deformation and induced surface charge. Since the induced potential is very sensitive to the distortion of the clay body, the simple shear plane test is more useful for understanding the characteristics of the charge distribution of SIP. The changes of SIP on each surface of a rectangular specimen with plane strain were recorded during the deformation test.

Test conditions

The plane shear test with a constant strain rate of 0.4%/min was performed under un-drained and atmospheric pressure conditions. External compressional force was applied to electrically isolated stainless steel loading plates at the upper and lower ends of a specimen to correspond with the

minimum strain axial plane. Here, tension is a positive value. A reference electrode was embedded in the center of the specimen. Thirty copper foil electrodes were mounted on both surfaces of the maximum principal axis plane. Twelve and twenty electrodes were also mounted on the surfaces of the intermediate and minimum axis planes, respectively. The size of each electrode was 5 mm x 5 mm. The variation of induced potential was recorded through a 16-bit, 1-Hz sampling A/D converter together with the vertical strain.

Specimen

Gouge blocks for the test specimen were cut out from an outcrop of the active Atotsugawa fault at Gifu Prefecture in central Japan. The gouge sample was remolded with saline water after screening out the coarse grains, and then consolidated axially under K_0 condition in a consolidation chamber 200 mm in inner diameter and 150 mm in height. The primary consolidation period was about 1000 min. and secondary compression was conducted at approximately 2000 min. The ultimate average void ratio was 2.18. A test specimen was removed from this chamber and formed into a rectangular prism 10.0 cm long, 3.0 cm wide and 5.0 cm high. The standing position of the specimen and the locations of the electrodes are shown in Fig. 1.

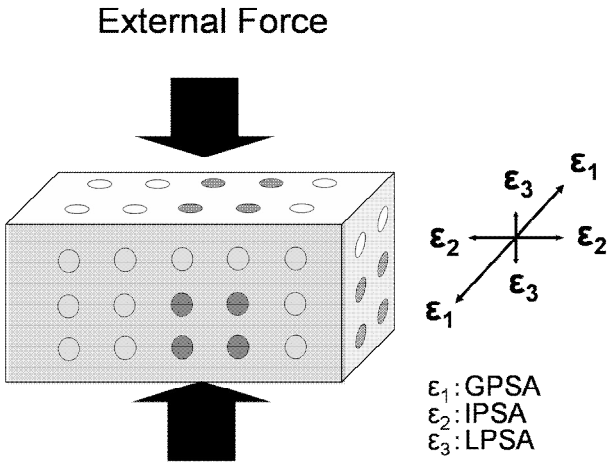

Fig. 1. Schematic diagram showing the simple plane shear test and the location of electrodes mounted on the surfaces of the specimen. The gray circles show the electrodes corresponding to those shown in Fig. 2. The orientation of each principal strain axis is shown in the legend on the right side. The abbreviations, GPSA, IPSA and LPSA represent the greatest, intermediate and least principal strain axes, respectively, in which the tension is positive.

Experimental result

Figure 2 shows a variation of the induced potential during shear deformation. For simplicity in showing the variation of the potential, only four traces for each surface of every plane are shown in the figure. There are rather large fluctuations in

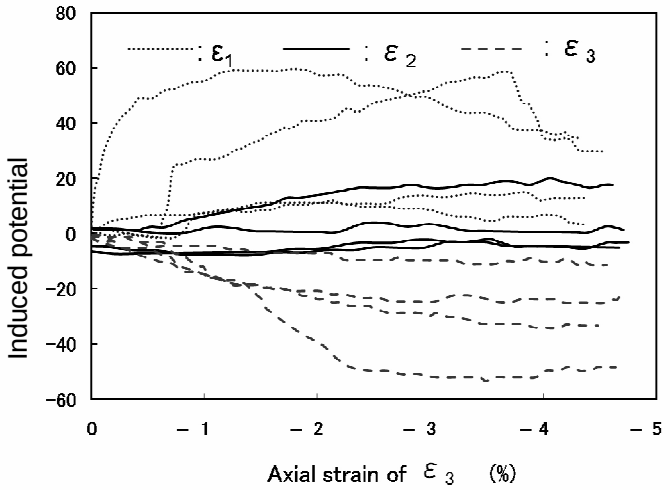

Fig. 2. An example of the variation of shear-induced potential with normal strain for the selected electrodes shown in Fig. 1. The axial strain is for the ε_3 plane (vertical compression). See Fig. 1 for the strain orientation.

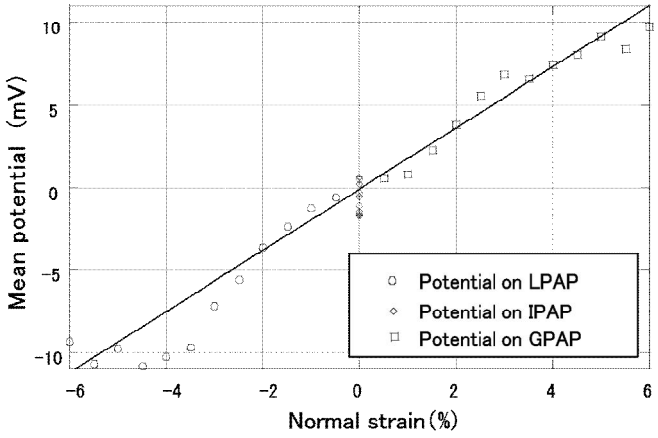

Fig. 3. Relationship between mean induced potential and normal strain of each axial plane. The normal strains of each plane were calculated from the vertical compressional strain assuming a constant specimen volume and uniform strain during deformation. See Fig. 1 for strain orientation.

the traces on the same plane. Four traces of the potential on the plane of the greatest strain axis indicate positive variations. Conversely, those on the plane of the least strain axis indicate negative variations and the potentials on the neutral plane do not vary by much at all. Assuming the constant volume of the specimen and the uniform strain during the shear deformation test, we can estimate each mean equivalent strain from the vertical axial strain. The relationship between the induced mean potential and strain is shown in Fig. 3. The mean potential can be calculated by averaging the potential of all electrodes on each plane. A positive proportional relationship characterizes the potential and normal strain. The proportional constant is evaluated as 1.91 volts per strain with a correlation coefficient of 0.988.

APPLICATION TO LANDSLIDES

The phenomenon of SIP may be used for monitoring symptoms of failure in a gouge, such as the fault sliding caused by an earthquake or mass movement. Accordingly, it is very important to verify the existence of SIP in actual geographic areas. However, since the generation of an earthquake is rare, it is difficult to inspect the detailed SIP from active faults. Alternatively, landslides offer better opportunities to examine this phenomenon. Two landslide sites, the Busuno and Nuta-Yone landslides, were selected to confirm the existence of SIP. Numerous observations of SP (spontaneous potential) were performed using observation networks of potential sensors which consisted of carbon electrodes 40 cm in length and 1.4 cm in diameter. The ground was drilled to a depth of 2 m to insert the electrode. A bentonite cake prepared with salt water was added to fill the drilled hole to decrease the contact resistance between the electrode and the wall of the hole. A PC with a built-in 16-bit A/D converter stored the value of SP together with the time.

Busuno landslide area

The Busuno landslide is located in the Chuetsu Mountains in Niigata Prefecture, Northeast Japan. The sliding rate of this area is one of the largest in Japan (Fig. 4). Many data of the landslide and meteorological have been obtained by the FFPR (Forestry and Forest Products Research Institute). This landslide mass is characterized by a weathered Tertiary formation that consists of alternating layers of coarse and medium sandy mudstones. In addition, the formation was tectonically deformed by folding. A total of 49 electrodes were embedded into the subsoil in the sliding mass with a larger slip rate to observe the SP. The observation area for the potential is shown by the rectangular area in Fig. 4. Almost all of the electrodes were set at 2 m in depth, and some at two or three locations were set at different depths to 3 m in the same hole for vertical array observation. Some cables connecting the electrodes were damaged severely by small animals such as moles or by unknown causes. The damage commonly results in a cutoff or short circuit, which causes a signal to be off the scale, null or remarkable unsteady. In this section, the data obtained from July 07, 2005 to November 18, 2005 were examined. The slip displacement of the sliding mass was also measured by the Institute of FFPR. Figure 5 shows the arrangements of sensors of the electrode and the displacement, and also shows a distribution of the polarity for the electric charges accumulated 78 days after start of the observation.

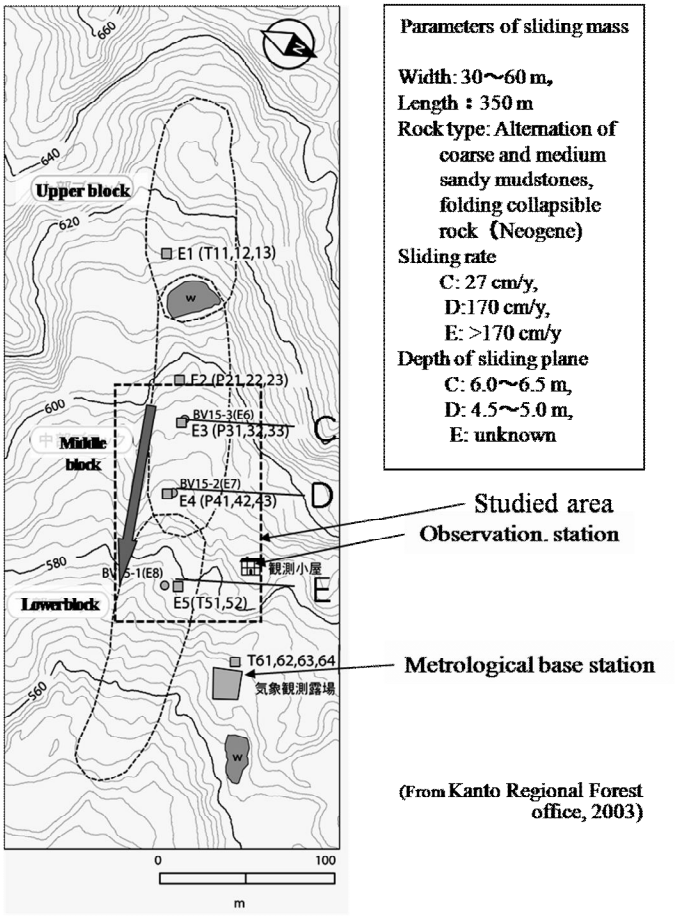

Fig. 4. Map of the landslide mass for the Busuno landslide in Niigata Prefecture, Northwest Japan. The studied area is indicated as the rectangular area formed by the dotted line.

Figures 6 and 7 are examples of the records of the potential and the slip displacement generated in the landslide masses. Conspicuous variations with time were found, as shown in the figures. There were two rainfalls during the first 12 days after beginning the observations. In general, there is a relatively strong correlation between SP and precipitation, so

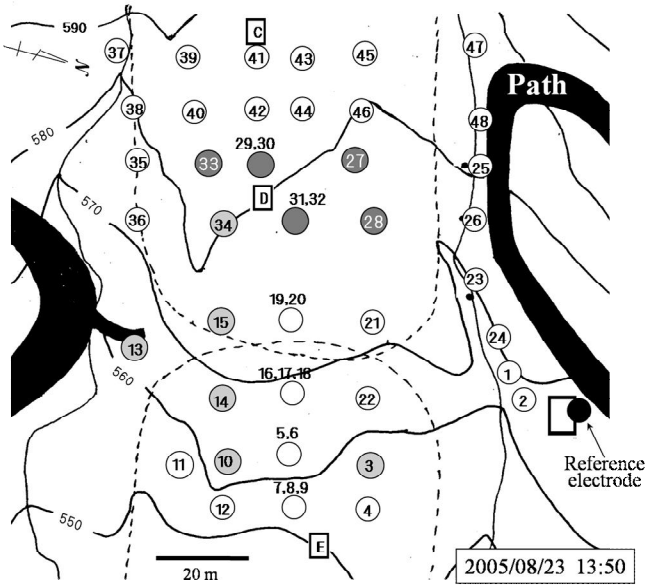

Fig. 5. Arrangement of electrodes in the Busuno landslide area, shown as the rectangular area in Fig. 4. The circled numbers are the electrode numbers. The dark and bright gray circles indicate the electrodes in which the potential changed to negative and positive values, respectively. Letters in rectangles are the stations for displacement measurements of the landslide.

that the streaming potential reflects directly the moisture migration.

The traces of SP with time, shown in Fig. 6, consist mainly of the high-frequency oscillation, daily variation and slow variation as seen in some types of relaxation. Associated with the precipitation, the SP changed with high-frequency ringing or pulse trains, as shown in Fig. 6. However, the landslide occurrence seems to be triggered by rainfall, as shown in the variations of the slip displacement with time in this figure. The typical forms of large variation of SP and slip displacement

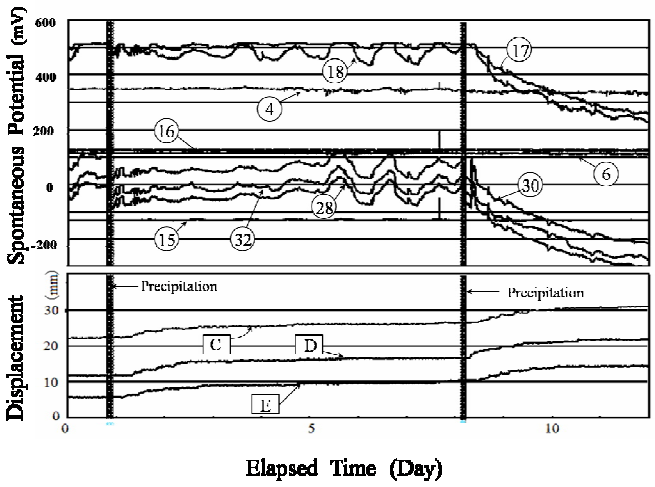

Fig. 6. An example of the variation with time of the spontaneous potential and the slip displacement recorded at the Busuno landslide area. The letter or number of each trace corresponds to those of Fig. 5. Note the spike-like changes of the potential corresponding to the precipitation.

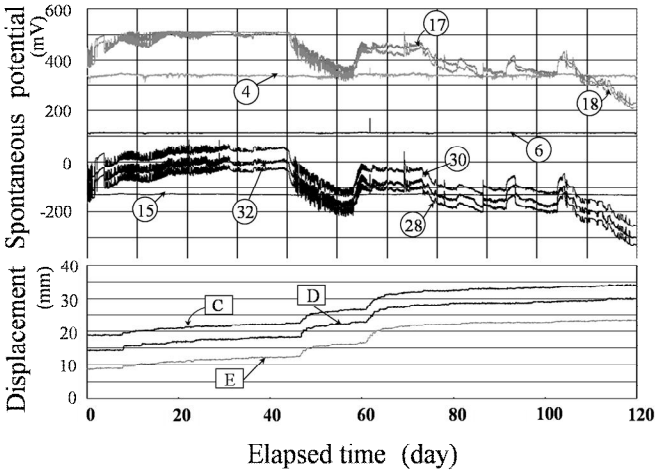

Fig. 7. An example of the variation of the spontaneous potential and the slip displacement with time recorded at the Busuno landslide area. The letter or number of each trace in the figure corresponds to that of Fig. 5. Notice the variation with time of the spontaneous potential corresponding to that of the slip displacement of the landslide.

with time after the second rainfall are very similar, but these phases are inverted. Accordingly, the direct variation of SP caused by the precipitation can be distinguished from that of the landslide. Figure 7 shows the SP and landslide variations with time for a longer period. The features of these two variations were not always similar, but the start of the SP events and the start of slip events were almost the same. Therefore, it can be considered that there is a clear cause-and-effect between SP and a landslide. According to the Institute of FFPR (2002), the sliding rate in this area has been high, as shown in Fig. 4. This area, however, was not as active at the time when our observation began. The slip displacement records of the C and D stations showed almost the same variation with time, and the variation was somewhat larger variation than that of the E station, as shown in Fig. 7. This means that the area located between stations D and E was shortened. The SP showed a higher value in this shortened area compared with the upper area, as shown in Fig. 5. This topic is discussed in a later section.

Nuta-Youne landslide area

The Nuta-Youne landslide is located in the mountains in Kochi Prefecture, Shikoku Island, southwest Japan. This landslide area is about 250 square km in area. This landslide mass is characterized by weathered pelitic schist that originated from the Mikabu tectonic belt. Figure 8 shows the topography and the distribution of the slip vector for each landslide mass. The slip rate of the landslide was determined by the Government Office of Kochi Prefecture. As in the previous figures, the rectangular area in the figure corresponds to the area studied. Figure 9 shows the arrangement of electrodes for the SP observation in the Nishikawa district.
The observation line of the electrode numbers from 21 to 28,

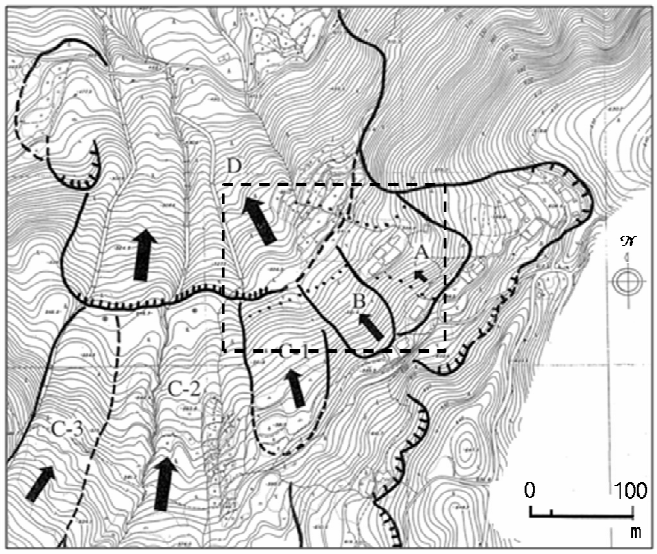

Fig. 8. Topography and slip sense of the Nishikawa district in the Nuta-Youne landslide province (from the Government Office of Kochi Prefecture). The rectangular area indicates the area studied.

which transverses the landslide masses of B and C-1, as shown in Fig. 9, was relatively accessible. According to the Government Office of Kochi Prefecture, the magnitudes of the slip rate of the B and C-1 sliding masses were estimated to be approximately 10 mm/year and approximately 20 mm/year, respectively. An example of the SP variation with time obtained along the observation line is shown in Fig. 10. The SP traces of all electrodes converged to a single curve within the first few hours after setting the electrode, and the converged state continued for approximately 24 hours with some variations. After the first day, however, these traces broadly diverged with time and somewhat monotonous variations, as shown in the figure. Although some form of

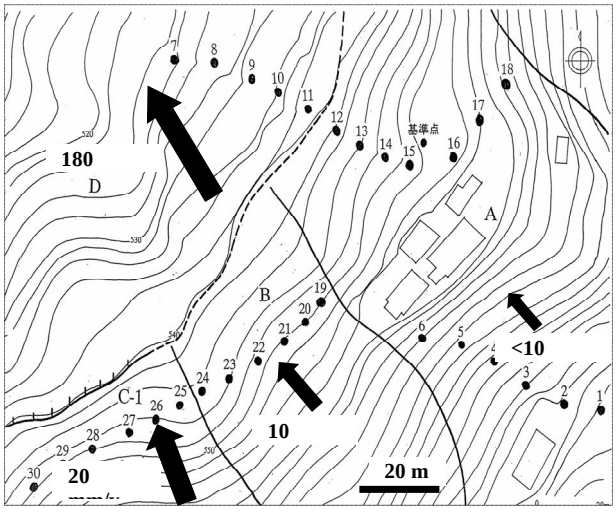

Fig. 9. Arrangement of electrodes at the Nishikawa district in the Nuta-Youne landslide shown as the rectangular area in Fig. 8. The numbered circles indicate the electrode number. Arrows indicate the slip direction and relative slip rate of the landslide block.

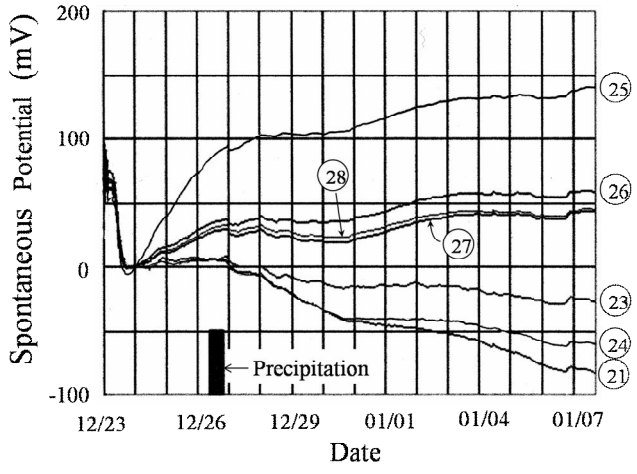

Fig. 10. An example of the variation of the spontaneous potential with time recorded at the Nishikawa district in the Nuta-Youne landslide. The number for each trace is the electrode number corresponding to that in Fig. 9.

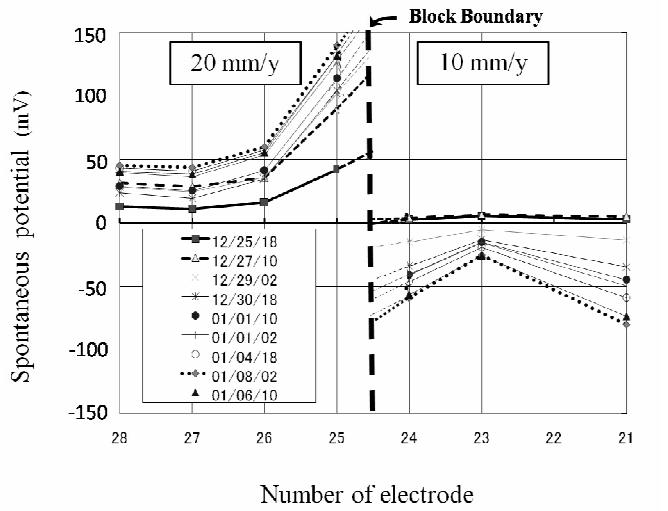

Fig. 11. Profile of the spontaneous potential across the boundary separating two landslide blocks with different slip rates at the Nishikawa district in the Nuta-Youne landslide area. Each plot indicates the potential for the electrode number at the time shown in the legend.

order rule was recognized between the slope of the traces and the number of electrodes, a very large gap existed between the electrode numbers of 24 and 25.

Figure 11 shows a profile of the SP distribution along the observation line of the electrode numbers from 21 to 28. Each trace of the profile has a distinctive discontinuity at the boundary separating the landslide masses of different slip rates. It is obvious that the magnitudes of offset at the discontinuity increased with elapsed time and the potential of the larger slip rate mass were higher than that of the smaller one.

Scaled model simulation

In order to examine the complicated results from the actual landslides, a scaled model simulation was performed in the laboratory. The material for the test specimen was collected from the gouge zone of granite on the Median Tectonic Line at Wakayama Prefecture, Southwest Japan. The material was sieved into fine-grained soil. Figure 12 shows a schematic diagram of the arrangements of the soil blocks and electrodes for the scaled model simulation of the landslide.

Three pieces of soil block were prepared for two sliding masses and one stable basement. Two sliding masses were put alongside on the stable bottom mass, and a thin lubricant soil layer was intercalated between the sliding masses and the bottom mass to make them slippery. The sliding mass can slide downward by inclining the bottom mass. Two linear voltage displacement transducers (LVDT) were set between the sliding masses and the bottom mass to monitor the amount of slip of the sliding masses. Twelve electrodes made by carbon rods were placed on the surface of each soil block, as

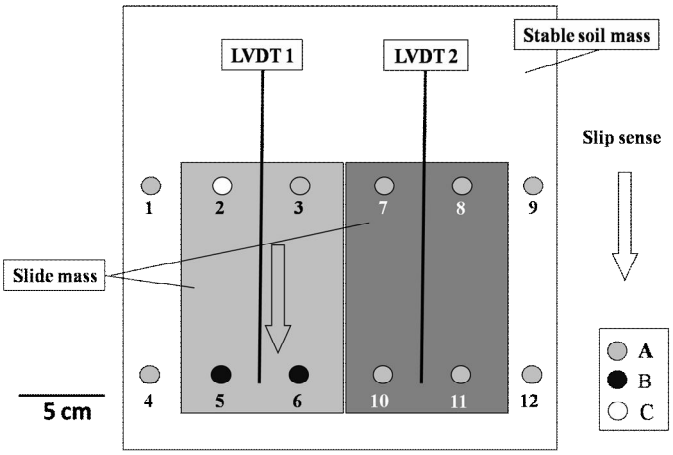

Fig. 12. Schematic diagram (plane view) showing the model for landslide simulation in the laboratory. Two unstable masses ride on a stable bottom mass. The unstable mass can slip downward to the bottom by lifting one of the edges (top of the figure) of the unstable masses. The light-gray unstable mass is made more slippery by a thin intercalated soft layer than that of the dark-gray mass. The numbered circles show the locations and number of the electrodes. A: electrode almost unchanged, B: electrode changed positively, C: electrode changed negatively.

shown in Fig. 12. An aluminum plate under the stable basement was utilized as the reference electrode.

Figure 13 shows an example of the time variations of the potential induced (SIP) in the soil masses by sliding and the slip displacement of the unstable sliding masses. For simplicity, five traces for the electrodes exhibiting the largest group of variation in SIP were selected. The number on both sides of each trace indicates the electrode or LVDT. As shown in the records of slip displacement, the sliding manner was somewhat different from that of the actual landslide shown in Figs. 6 and 7. The slip was a stick-slip note, not a smooth

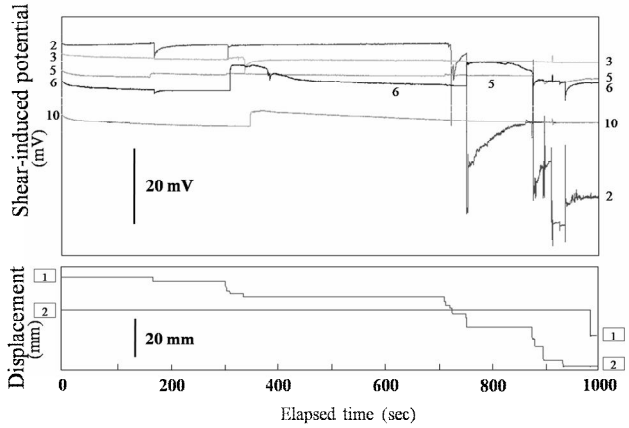

Fig. 13. Time variations of the SIP (upper) and slip displacement (lower) by the simulation of the scaled model for the Nishikawa district in the Nuta-Youne landslide. The number of each trace shows the number of the electrode or displacement sensor (LVDT).

creep type. However, it is obvious that the electric potential rapidly varied according to the slip of the sliding mass. The most sensitive electrode (No. 2) decreased about 40 mV with a displacement of about 50 mm. The gradual variation of the potential during the period from 0 to 150 sec in elapsed time is considered to result from plastic deformation by the shear stress, which was generated in the inclined soil mass under the gravitational force. One of the most characteristic features of these SIP traces is a spike-like variation, which coincides synchronously with the first kick of the stick-slip for sliding. Another feature is a subsequent special form to the spike-like variation, which suggests some kind of relaxation process. The maximum variation of the SIP reached the order of several tens of milli-volts.

DISCUSSION

It was clarified that some kind of charge polarization in the fine soil body is induced by the deformation. This phenomenon could be found not only in the laboratory simulation but also in the field experiments. It is confirmed by the similarity between the variations of the potential and strain.

The plane strain test showed that positive charges accumulated on the surface of the greatest principal strain axial plane (extensional axial plane), as shown in Figs. 2 and 3. The detailed mechanism of the polarization associated with the shear deformation is not clear. However, it can be hypothesized that breaking the inter-particle bonding by deformation disturbs the electric equilibrium near the particle contacts and subsequently releases the semi-ordered cations from the adsorbed layer into the free pore water. A possible model of this idea is shown in Fig. 14. The experimental results and the simulation described above suggest that the movement of the electric positive charge is apparently in agreement with the movement of the grains by deformation. The characteristic distribution of the polarity of SP was found in the unstable block in the Busuno landslide area. Electrodes were set up across the boundary of the landslide blocks. Because the slip rates of two observation points, C and D, located in the middle block, were nearly equal, as shown in Figs. 6 and 7, the middle block is assumed to have slid

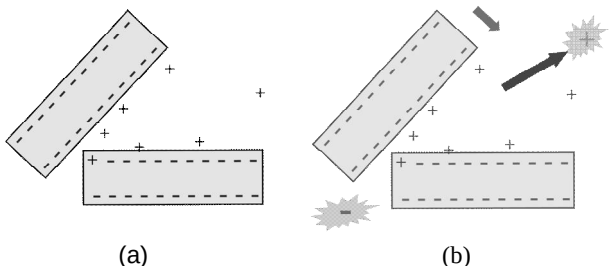

Fig. 14. A schematic model for the distribution of electric charge near the particle contact in the clay-electrolyte-water system. (a): Distribution of electric charge in the equilibrium state, (b): Electric polarization resulting from the structural deformation.

uniformly as a block during the observation period. However, as the slip rate at the lowest observation point was significantly smaller than that of the other two stations, the lowest block is assumed to have had a decrease in activity. Accordingly, from the polarity distribution shown in Fig. 5, it can be explained that the positive charges and negative charges accumulated at the front and rear parts of the landslide mass, respectively.

In the case of the Nishikawa district in the Nuta-Youne landslide, electrodes for the SP observation were arranged across the mass boundary, which is parallel to the slip direction and separates the masses of different slip rates. The distribution of SP shows a large discontinuity at the boundary. The discrepancy between the SP values at both sides of the boundary increased with time, as shown in Fig. 11. The polarity of the mass with a larger slip rate was positive and that of the smaller one was negative. Accordingly, this means that the potential of the larger slip rate mass showed a relatively higher potential. As the absolute value of SP depends on the location of the reference electrode, the absolute value itself is meaningless.

The result of the experiment shown in Fig. 12 to verify the characteristic feature of SP of the landslide in the actual field strongly supports the interpretation mentioned above. The potentials of the electrodes (Nos. 5 and 6) located at the front of the unstable mass also show higher a potential compared than that of the rear (Nos. 2 and 3).

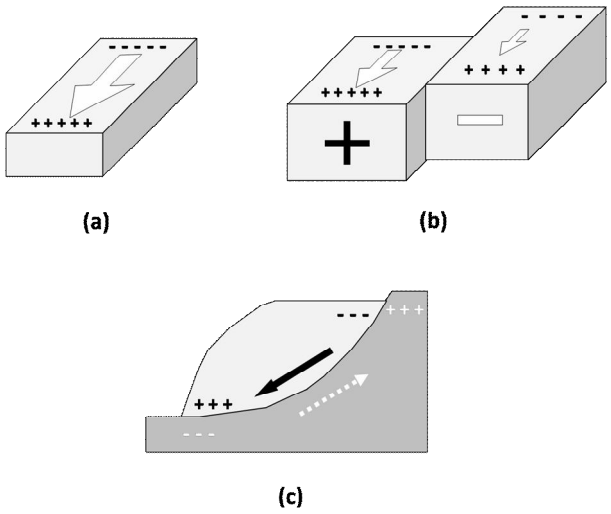

Fig. 15. Schematic diagram showing the typical polarity pattern of the induced electric charges accompanying the two landslides. The arrows show the sense and relative magnitude of the slip displacement of the landslide. (a): Polarity pattern of SP appearing in the Busuno landslide, (b): Polarity pattern of SP appearing in the Nuta-Youne landslide (Nishikawa area), (c): Generalized polarity model of SP or SIP induced in the unstable and stable masses accompanying the landslides.

To summarize our interpretation of the results obtained from the field and the laboratory, we can present a conceptual picture, as shown in Fig. 15. The upper diagrams (a) and (b) in this figure show the models appearing in the field of the Busuno landslide and Nuta-Youne landslide. These patterns were also observed in the laboratory. The bottom diagram (c) is a generalized image on the polarity pattern of SIP expected in the landslide area.

We sometimes observed some SIP or SP events not corresponding to the slip events recorded by displacement sensors, as shown in Figs. 7 and 13. These results suggest that SIP is detectable for the local strain by deformation, but, on the contrary, the general displacement sensor is not sensitive to microscopic or local strain but averaged strain. Since SIP or SP is a good indicator for detecting the microscopic strain change as long as most noises can be excluded, it becomes a helpful tool to monitor the symptoms of failure.

CONCLUSIONS

The relationships between the electric potential induced on the surface of a fine soil block and the deformation was clarified in laboratory tests. We called this potential the shear-induced potential, SIP. The magnitude of SIP for some types of gouge material was experimentally estimated to 1.91 volts per strain.

The result of the plane strain test showed that the greatest principal axial plane surfaces were positively charged and the least principal axial plane surfaces were negatively charged. This characteristic feature was interpreted as follows: breaking the inter-particle bonding by deformation disturbs the electric equilibrium near the particle contacts and subsequently releases the semi-ordered cations from the adsorbed layer into the free pore water.

The close relationship between the spontaneous potential and the slip of landslide was clarified from two observation fields. This relationship was verified in the laboratory. A polarity model explaining the distribution of the charges observed was presented.

It is ultimately concluded that observation of the spontaneous potential can be an effective method to monitor the symptoms of a failure such as a landslide or an earthquake.

ACKNOWLEDGMENTS

The authors are indebted to Professor James K. Mitchell of Virginia Polytechnic Institute and Professor Kenichi Soga of the University of Cambridge for their valuable discussions on inter-particle bonding. We would like to Dr. Takashi Okamoto of the Forestry and Forest Products Research Institute for his helpful advice and providing information on landslides. The authors are also grateful to Mr. Akira Okamoto and his family at Otoyo-cho for their providing their facility for observation.

Part of this research was supported by a Grant-in-Aid for scientific research from Japan Society for the Promotion of Science.

REFERENCES

Kanto Regional Forest Office (2003), "Investigation on deformation mechanism of landslide."

Kazintsev, E.A. (1968), "Pore solutions of Maykop Formation of Eastern Pre-Caucasus and method of squeezing of pore waters at high temperatures," *Compaction of argillaceous sediments*, (H.H. Rieke III and G.V. Chilingarian, ed., 1974) Elsevier, New York.

Mitchell, J.K. and Soga K. (2005), "*Fundamentals of soil behavior*", 3rd Ed., John Wiley & sons, New York.

Nakagawa, K., Soga, K., Mitchell, J. K. and Sadek, M. S. (1995), "Soil structure changes during and after consolidation as indicated by shear wave velocity and electrical conductivity measurements," In *Proc. Int., Symp. on Compression and Consolidation of Clayey Soils*, Hiroshima, pp. 229-234.

Sawabini, C.T., Chilingarian, G.V. and Rieke, H.H., (1972), "Effect of compaction on chemistry of solution expelled from montmorillonite clay saturated in sea water," *Compaction of argillaceous sediments*, (H.H. Rieke III and G.V. Chilingarian, ed., 1974) , Elsevier, New York.